SLAC – PUB – 4441
November 1987
(A)

WAKEFIELDS OF VERY SHORT BUNCHES IN AN ACCELERATING CAVITY*

KARL BANE AND MATTHEW SANDS

Stanford Linear Accelerator Center

Stanford University, Stanford, California, 94305

ABSTRACT

The behavior of the longitudinal and transverse wakefields of short bunches in an accelerating cavity has been examined. Computations of short time wakefields have been carried out using T. Weiland's computer program TBCI,[1] which integrates Maxwell's Equations in the time domain. We present also our version of the diffraction model of the high frequency impedance of the cavity, a model originally suggested by Lawson.[2] This model predicts a longitudinal impedance that varies as $\omega^{-1/2}$ and a transverse impedance that varies as $\omega^{-3/2}$ at high frequencies, with their ratio equal to $\omega a^2/(2c)$, where a is the radius of the beam tube. We find that as shorter bunches are used, the computations approach asymptotically the predictions of the diffraction model. These asymptotic wakes are also in accord with calculations of Dôme[3] and of Heifets and Kheifets.[4]

---

* Work supported by the Department of Energy, contract DE – AC03 – 76SF00515.

Presented at the Workshop on Impedances Beyond Cut-off, Berkeley, Ca., August 18–21, 1987

TABLE OF CONTENTS

1. Introduction

Recent studies of possible future linear colliders have shown that it may be desirable to accelerate exceedingly short bunches.[5,6] As an example, J. Rees[6] has presented a consistent set of parameters for a 1 TeV collider which includes a bunch length of 3×10^{-6} meter – about 300 times shorter than the bunch length of the Stanford Linear Collider.

The performance of such a collider will depend critically on the details of the electro-magnetic interaction of the bunch with the accelerating structure – that is, on the so-called wakefields. These wakefields give rise to a parasitic energy loss of the bunch, to an induced energy spread of the electrons in the bunch, and to transverse forces that tend to increase the effective beam emittance. It appears that if we want to contemplate seriously the design of any future collider, we will need to understand the nature of the wakes of very short bunches – bunches which are orders of magnitude shorter than any of the characteristic lengths of a typical accelerating cavity.

As a first step we consider, in this report, the wakefields of short bunches in an accelerating cavity consisting of a pillbox with infinitely long beam tubes (see Fig. 1). We will consider the problem of a periodic structure in a future paper. We begin this report by introducing our notation, and reviewing some properties of wake functions and impedances. Then we discuss the relationship between wakes of short bunches and the impedances at high frequencies. We then look at the high-frequency behavior of wakes that is predicted by a diffraction model, first suggested by J. Lawson.[2] We give our version of this model in detail in Appendix A. Finally we present results of computations using the code TBCI[1] to obtain the wakefields of short gaussian bunches in our model structure, and

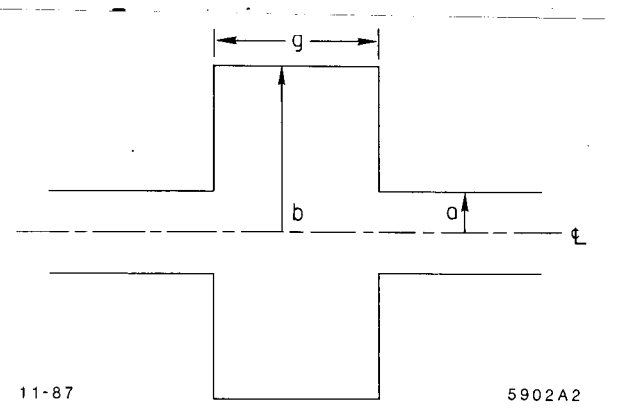

Fig. 1. Our model structure: a single pillbox cavity with infinitely long beam tubes.

compare these results with predictions of the diffraction model.

2. Wakes and Impedances

We review here some definitions of wakes and impedances and introduce our notation. For a more thorough discussion of the properties of wakefields see, for example, the lectures by Bane, Weiland, and Wilson.[7]

2.1 Longitudinal Wakes

When an ultra-relativistic bunch containing a total charge Q passes along the axis of a cylindrically-symmetric cavity, a wake field is generated which will extract the energy $\Delta U(s)$ from any small "test" charge q that travels with the bunch some longitudinal distance s from a reference point in the bunch – say, the bunch center. We take s to be *positive* toward the *rear* of the bunch. It is convenient to define the longitudinal wake function $W_{\parallel}(s)$ as that energy loss per unit of both charges, namely by

$$W_{\parallel}(s) = \frac{\Delta U(s)}{qQ} \quad . \tag{2.1}$$

We will write $W_{\|0}(s)$ to represent the "impulse" wake function, namely the one for a point-like bunch. For all practical purposes, the impulse wake for highly relativistic bunches is zero for all negative s; then the longitudinal wake function for an arbitrary bunch whose longitudinal charge density is $\lambda(s)$ can be expressed, in terms of $W_{\|0}$, by

$$W_{\|}(s) = \frac{1}{Q}\int_0^\infty \lambda(s-s')\,W_{\|0}(s')ds' \quad . \tag{2.2}$$

It is often useful to characterize the longitudinal wake in terms of a longitudinal impedance $Z_{\|}(\omega)$ which is, effectively, the Fourier-transform of $W_{\|0}(s)$

$$Z_{\|}(\omega) = \frac{1}{c}\int_0^\infty W_{\|0}(s)\,e^{i\omega s/c}ds \quad . \tag{2.3}$$

We will call the real and imaginary parts of the impedance the wake "resistance" $\mathcal{R}_{\|}(\omega)$ and "reactance" $\mathcal{X}_{\|}(\omega)$:

$$Z_{\|}(\omega) = \mathcal{R}_{\|}(\omega) + i\mathcal{X}_{\|}(\omega) \quad . \tag{2.4}$$

The total energy lost by a bunch of unit charge during one passage through a cavity is called the loss factor $k_{\|}$, and can be expressed in terms of an integral over the wake function or, alternatively, over the cavity resistance:

$$\begin{aligned} k_{\|} =& \frac{1}{Q}\int_{-\infty}^\infty \lambda(s)\,W_{\|}(s)\,ds \\ =& \frac{1}{\pi Q^2}\int_0^\infty \tilde{\lambda}^2(\omega)\,\mathcal{R}_{\|}(\omega)\,d\omega \quad , \end{aligned} \tag{2.5}$$

where $\tilde{\lambda}(\omega)$ is the Fourier-transform of $\lambda(s)$. We will here be considering only

gaussian bunches. For such a bunch, with an r.m.s. length σ,

$$\begin{aligned} k_{\|}(\sigma) &= \frac{1}{\sqrt{2\pi}\sigma} \int_{-\infty}^{\infty} W_{\|}(s,\sigma) e^{-s^2/2\sigma^2} ds \\ &= \frac{1}{\pi} \int_{0}^{\infty} \mathcal{R}_{\|}(\omega) e^{-(\omega\sigma/c)^2} d\omega \quad , \end{aligned} \tag{2.6}$$

where $W_{\|}(s,\sigma)$ is the wake function of a gaussian bunch. Notice that because $\mathcal{R}_{\|}$ is positive definite, $k_{\|}$ is a monotonically decreasing function of σ.

2.2 Transverse Wakes

Now suppose a bunch passes through a cylindrically-symmetric cavity at a small transverse displacement x with respect to the cavity axis. Then the wake-fields produced exert a transverse force on accompanying particles that depends on x as well as s. We will focus our attention here on the total transverse impulse $\Delta p_x(s)$ received by a test charge q which accompanies the bunch at the longitudinal position s with respect to the bunch center. If the bunch displacement is small, only the so-called dipole part of the transverse wake is significant, and $\Delta p_x(s)$ is proportional to the bunch displacement x and independent of the transverse position of the test charge. Then it is convenient to define a transverse wake function $W_{\perp}(s)$ by

$$W_{\perp}(s) = \frac{c\Delta p_x(s)}{qQx} \quad . \tag{2.7}$$

Again, we can relate $W_{\perp}(s)$ to the impulse wake $W_{\perp 0}(s)$ (from a point-like bunch) with a convolution integral corresponding to Eq. (2.2). And the trans-

verse impedance function $Z_\perp(\omega)$ is defined by

$$Z_\perp(\omega) \;=\; \mathcal{R}_\perp(\omega) + i\mathcal{X}_\perp(\omega) \;=\; -\frac{i}{c}\int_0^\infty W_{\perp 0}(s)e^{i\omega s/c}\,ds \quad . \tag{2.8}$$

By tradition the negative imaginary unit is introduced in the definition of $Z_\perp(\omega)$ so that $Z_\perp$ and $Z_\parallel$ appear in quite similar ways in the calculations of transverse and longitudinal instabilities.

It is also useful to define a transverse impulse factor $k_\perp$ for a bunch offset from the axis by a fixed amount as c/Q^2 times the total transverse momentum given to the bunch by its own wake. It is obtained from an integral over the wake function or over the impedance analogous to one of those in Eq. (2.5). For a gaussian bunch

$$\begin{aligned} k_\perp(\sigma) =& \frac{1}{\sqrt{2\pi}\sigma}\int_{-\infty}^\infty W_\perp(s,\sigma)e^{-s^2/2\sigma^2}\,ds \\ =& -\frac{1}{\pi}\int_0^\infty \mathcal{X}_\perp(\omega)e^{-(\omega\sigma/c)^2}\,d\omega \quad . \end{aligned} \tag{2.9}$$

Due to the negative imaginary unit introduced in the definition of $Z_\perp(\omega)$ it is the transverse reactance, rather than the transverse resistance, that is found in the above equation. The reactance can be written in terms of the resistance by the use of the Hilbert transform[8]

$$\mathcal{X}_\perp(\omega) = -\frac{1}{\pi}\fint_{-\infty}^\infty \frac{\mathcal{R}_\perp(\omega')}{\omega'-\omega}\,d\omega' \quad , \tag{2.10}$$

with the symbol $\fint$ indicating that the integral is performed as a Cauchy principal value. Substituting Eq. (2.10) into the second integral of Eq. (2.9), and then

reversing the order of integration we find that

$$k_\perp(\sigma) = \frac{2}{\pi^{3/2}} \int_0^\infty \mathcal{R}_\perp(\omega) D(\omega\sigma/c)\, d\omega \quad , \tag{2.11}$$

with $D(x)$, known as Dawson's integral, given by

$$D(x) = e^{-x^2} \int_0^x e^{y^2}\, dy \quad . \tag{2.12}$$

We see that the transverse impulse factor $k_\perp(\sigma)$ can be expressed as an integral over the transverse resistance $\mathcal{R}_\perp(\omega)$, but with an "effective" spectrum given by the Dawson Integral $D(\omega\sigma/c)$. It is easy to see that $D(x) \approx x$ when x is small, whereas $D(x) \approx 1/(2x)$ when x becomes large. A plot of Dawson's integral is given in Fig. 2, where we show for comparison also the corresponding bunch spectrum e^{-x^2}.

For physical reasons $\mathcal{R}_\perp(\omega)$ will be positive for positive values of ω, will be finite for small ω, and will tend toward zero for large ω. Given these facts and the form of Dawson's integral it follows that $k_\perp(\sigma)$ is also positive definite, and approaches zero for very small, as well as very large, values of σ.

It is sometimes convenient to make use of the so-called *dipole* longitudinal wake function $W_\parallel^{(1)}(s)$ which can be defined by

$$W_\parallel^{(1)}(s) = \frac{d}{ds} W_\perp(s) \quad . \tag{2.13}$$

See, for example, Bane, *et. al.*[7] It can be shown from Maxwell's Equations that $W_\parallel^{(1)}$ describes the *longitudinal* forces associated with the transverse wakefield –

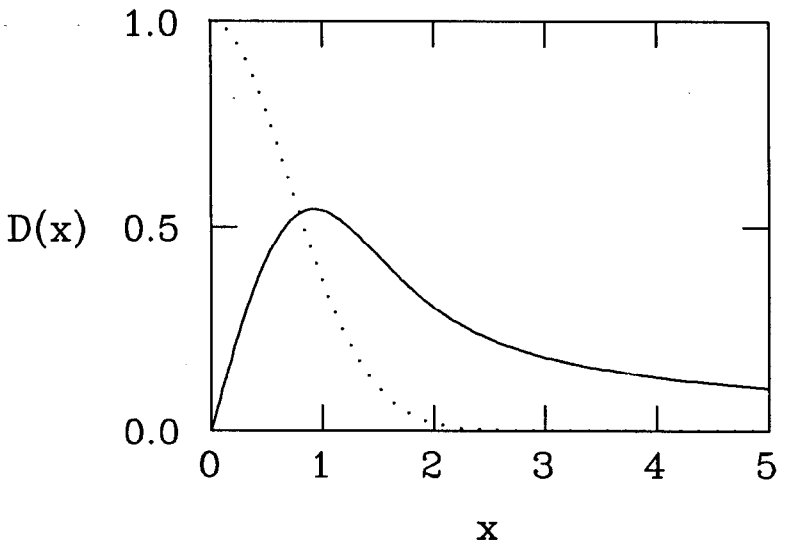

Fig. 2. Dawson's integral. For comparison, the factor e^{-x^2} is given by the dotted curve.

from which its name. It turns out that the test charge q (which accompanies the bunch at the same transverse displacement x) loses the energy

$$\Delta U^{(1)}(s) = x^2 q Q W_{\parallel}^{(1)}(s) \quad . \tag{2.14}$$

The relationship between $\Delta U^{(1)}$ and $W_{\perp}$, obtained by combining Eqs. (2.13) and (2.14), is often referred to as the Panofsky-Wenzel Theorem.[9]

The dipole longitudinal impedance $Z_{\parallel}^{(1)}(\omega)$ and the dipole loss factor $k_{\parallel}^{(1)}$ are defined in terms of $W_{\parallel}^{(1)}(s)$ as in Eqs. (2.3) and (2.5). And it follows from these definitions that

$$Z_{\parallel}^{(1)}(\omega) = \frac{\omega}{c} Z_{\perp}(\omega) \quad . \tag{2.15}$$

We should emphasize that there is, in general, no necessary connection between the dipole longitudinal impedance $Z_{\parallel}^{(1)}(\omega)$ and the longitudinal impedance

$Z_{\|}(\omega)$ defined earlier. As we will see later, however, it turns out that the *high-frequency* behavior of the two impedances (and so of the corresponding wake functions) in a cavity are very closely connected.

* * *

Note that when speaking of the impedances in what follows, we will choose to limit our interest to the resistive parts. The imaginary parts can always be obtained from the resistive parts by means of the Hilbert transform.

3. Asymptotic Relations

The behavior of the wake functions of short bunches and of the cavity impedances at high frequencies are, of course, intimately related. We develop here some of these relations.

In a single cavity the resistance $\mathcal{R}(\omega)$ (either longitudinal or transverse) will, generally, have a number of sharp peaks (corresponding to resonances) at frequencies below the cut-off frequency ω_c of the beam pipe. At higher frequencies the natural cavity resonances are damped by radiation down the beam pipe; the resonances are broadened and the impedance tends to become relatively smooth – especially for frequencies well above ω_c. Since we are, here, only interested in the very short-time behavior of the wakefields of gaussian bunches, we need not be concerned with any rapid variations of $\mathcal{R}(\omega)$, and can be content with describing the "average" or "smoothed" behavior of the resistance. The $\mathcal{R}(\omega)$ we use here *will refer to such a smoothed function* – which is often called "the broad-band impedance". Speaking roughly, so long as we are only interested in the behavior of wake functions over a time interval ΔT we may take $\mathcal{R}(\omega)$ to be a running average with a "bin width" $\Delta\omega$ of about $2\pi/\Delta T$. Since we are here

interested in a ΔT which is generally only some factor like, say, 6 larger than σ/c, we may think of the smoothing width $\Delta\omega$ as the order of c/σ.

As we will see, various methods of calculating the high frequency resistance yield results that decrease as some power of the frequency, and in this case the relations among the various wake-related functions become particularly simple. Lets look first at the longitudinal wakes.

3.1 The Relation Between $k_{\|}(\sigma)$ and $\mathcal{R}_{\|}(\omega)$

If we know the longitudinal resistance $\mathcal{R}_{\|}(\omega)$ for all frequencies we can find the loss factor $k_{\|}(\sigma)$ for all σ by a numerical integration of Eq. (2.6). If, however, we know only the high frequency part of the impedance we can still obtain information about $k_{\|}(\sigma)$ for short bunches. And, alternatively, knowing $k_{\|}(\sigma)$ for short bunches gives us information about the broad-band or "smoothed" impedance at high frequencies. We can get some insight into the general nature of the relationship between $\mathcal{R}_{\|}(\omega)$ for large ω and $k_{\|}(\sigma)$ for small σ from the following simple argument. Suppose that we approximate the integral of Eq. (2.6) by replacing the exponential factor in the integral with the rectangular function which is equal to 1 out to $\omega = c/\sigma$ and to 0 beyond. Then we have

$$k_{\|}(\sigma) \approx \frac{1}{\pi} \int_0^{c/\sigma} \mathcal{R}_{\|}(\omega)\, d\omega \quad . \tag{3.1}$$

If we differentiate Eq. (3.1) with respect to σ we get the following heuristic relationship between $k_{\|}$ and $\mathcal{R}_{\|}$:

$$\left(\frac{\pi\sigma^2}{c}\right) \frac{dk_{\|}(\sigma)}{d\sigma} \approx -\mathcal{R}_{\|}(c/\sigma) \quad . \tag{3.2}$$

Knowing $k_{\|}$ in the neighborhood of some particular σ gives us information of the

broad-band impedance at $\omega = c/\sigma$.

From Eq. (3.1) we see that if $\mathcal{R}_\parallel(\omega)$ falls off faster than $1/\omega$ at high frequencies, then $k_\parallel(\sigma)$ will approach some finite value k_0 as σ goes toward zero. If, however, $\mathcal{R}_\parallel(\omega)$ decreases more slowly than $1/\omega$, then $k_\parallel(\sigma)$ will increase without limit as σ goes to zero; and the asymptotic behavior of $k_\parallel(\sigma)$ for small σ will be determined by the high frequency part of the impedance.

If we know that $\mathcal{R}_\parallel(\omega)$ has some specific form at high frequencies we can be more precise. Suppose that $\mathcal{R}_\parallel(\omega)$ can be described for frequencies above some transition frequency ω_t by

$$\mathcal{R}_\parallel(\omega) = A\omega^{-\alpha} \qquad (\omega > \omega_t) \quad . \tag{3.3}$$

We then consider the second integral of Eq. (2.6) in two parts: the part $k_{\parallel 1}$ for frequencies below ω_t and the part $k_{\parallel 2}$ for frequencies above ω_t. The first part $k_{\parallel 1}$, which characterizes the low-frequency structure of the cavity is finite and will approach some constant number once σ is less than c/ω_t. If $\alpha > 1$ the second part $k_{\parallel 2}$ will also approach, for small σ, some constant value, which will add to $k_{\parallel 1}$ to give a $k_\parallel(\sigma)$ that is also constant.

Suppose, however, that $0 < \alpha < 1$. Substituting Eq. (3.3) into Eq. (2.6) yields

$$k_{\parallel 2} = \frac{A}{\pi}\left(\frac{c}{\sigma}\right)^{1-\alpha} \int_{\omega_t\sigma/c}^{\infty} e^{-x^2} x^{-\alpha}\, dx \quad . \tag{3.4}$$

The integral above is the incomplete gamma function. For sufficiently small σ we can approximate $k_{\parallel 2}$ by

$$k_{\parallel 2} = \frac{A}{2\pi}\left(\frac{c}{\sigma}\right)^{1-\alpha}\left[\Gamma\left(\frac{1-\alpha}{2}\right) - \frac{2}{1-\alpha}\left(\frac{\omega_t\sigma}{c}\right)^{1-\alpha}\right] \qquad (\alpha < 1,\ \sigma \text{ small}), \tag{3.5}$$

where $\Gamma(x)$ is the usual gamma function. For σ sufficiently small, we can neglect the second term in Eq. (3.5). And since the remaining term increases without limit as σ goes toward zero, $k_{\|2}$ will ultimately dominate over the constant part $k_{\|1}$. It can then be used to approximate $k_{\|}(\sigma)$. Thus

$$k_{\|}(\sigma) = \frac{A}{2\pi}\Gamma(\frac{1-\alpha}{2})\left(\frac{c}{\sigma}\right)^{1-\alpha} \qquad (\alpha < 1, \sigma \text{ small}) \quad . \tag{3.6}$$

When $\alpha < 1$ the longitudinal resistance at high frequencies determines uniquely the loss factor for small σ; and it follows also if $k_{\|}(\sigma)$ varies as $\sigma^{\alpha-1}$ for small σ, $\mathcal{R}_{\|}(\omega)$ varies as $\omega^{-\alpha}$ at high frequencies.

3.2 The Relation Between $k_{\perp}(\sigma)$ and $\mathcal{R}_{\perp}(\omega)$

As we saw for the longitudinal wakes, the transverse impulse factor $k_{\perp}(\sigma)$ at small σ can be related to the broad-band behavior of $\mathcal{R}_{\perp}(\omega)$ at high frequencies. To examine the asymptotic relationship we will take that $\mathcal{R}_{\perp}(\omega)$ falls off as some power β of ω, for ω larger than a transition frequency ω_r; specifically we set

$$\mathcal{R}_{\perp}(\omega) = B\omega^{-\beta} \qquad (\omega > \omega_r) \quad . \tag{3.7}$$

Note that $\mathcal{R}_{\perp}(\omega)$ must decrease at large ω faster than ω^{-1}. With any slower fall-off, the energy loss from the dipole moment of a bunch would be infinite, which is non-physical. Therefore β must be greater than 1.

Consider now Eq. (2.11) which gives the transverse impulse factor of a gaussian bunch in terms of an integral over the transverse resistance. Again we may divide Eq. (2.11) into a low frequency part $k_{\perp 1}$, for frequencies below ω_r, and a high frequency part $k_{\perp 2}$, for frequencies above ω_r. When σ is much less than c/ω

we may use the small argument approximation for $D(x)$ – namely $D(x) \approx x$ – and then the low frequency part can be approximated by

$$k_{\perp 1} = \frac{2}{\pi^{3/2}} \left(\frac{\sigma}{c}\right) \int_0^{\omega_r} \mathcal{R}_\perp(\omega)\omega \, d\omega \qquad (\sigma \text{ small}) \quad . \tag{3.8}$$

Then when σ is small $k_{\perp 1}$ will approach some constant number times σ.

The behavior of the high frequency part $k_{\perp 2}$ depends on whether β is greater or less than 2. When $\beta > 2$ the high frequency part $k_{\perp 2}$ will also vary linearly with σ, when σ is small, and the total $k_\perp(\sigma)$ will also be proportional to σ.

When $\beta < 2$, however, the second part $k_{\perp 2}$ of the impulse factor can be written, for small σ, as

$$k_{\perp 2} = \frac{2B}{\pi^{3/2}} \left(\frac{1}{2-\beta}\right) \left(\frac{\sigma}{c}\right)^{\beta-1} \left[f(\beta) - \left(\frac{\omega_r \sigma}{c}\right)^{2-\beta}\right] \qquad (\beta < 2, \, \sigma \text{ small}) \quad , \tag{3.9}$$

where the first term in the square brackets $f(\beta)$ is

$$f(\beta) = (2-\beta) \int_0^\infty D(x) x^{-\beta} \, dx \quad , \tag{3.10}$$

and the second term just subtracts off that part of the same integral below ω_r (we have again used the small x approximation for $D(x)$). The function $f(\beta)$ can be evaluated numerically. It is approximately equal to 1, varying from 1.39 at $\beta = 1$, to 1.09 at $\beta = 3/2$, to 1.00 at $\beta = 2$. We see that for sufficiently small σ the first term in Eq. (3.9) will dominate over the second term, as well as over the contribution of $k_{\perp 1}$. Then we can approximate

$$k_\perp(\sigma) = \frac{2Bf(\beta)}{\pi^{3/2}} \left(\frac{1}{2-\beta}\right) \left(\frac{\sigma}{c}\right)^{\beta-1} \qquad (\beta < 2, \, \sigma \text{ small}) \quad . \tag{3.11}$$

We see there is a direct connection between the high frequency transverse resis-

tance and the transverse impulse factor for small σ.

3.3 The Diffraction Model: The Longitudinal Wakes

In 1968 J. Lawson[2] applied the methods of optical diffraction theory to calculate the energy loss of a point bunch passing through a single accelerating cavity. We believe that these methods can be used to obtain a reasonable estimate of the high-frequency part of the longitudinal resistance of a cavity. We will call such a calculation *the diffraction model.* Inasmuch as the original Lawson paper is not generally available, we present our version of the model in some detail in Appendix A. We also show there how the model can be extended to give the transverse resistance.

According to the diffraction model – see Eq. (A.8) in Appendix A – the wake resistance of a cavity at high frequencies is

$$\mathcal{R}_{\parallel}(\omega) = \frac{Z_0}{2\pi^{3/2}}\sqrt{\frac{cg}{a^2\omega}} \quad , \tag{3.12}$$

with $Z_0 = 377\,\Omega$, the impedance of free space, and a and g are the cavity dimensions as shown in Fig. 1. The diffraction model gives for the $\mathcal{R}_{\parallel}(\omega)$ of a single cavity with beam tubes a high frequency dependence of $\omega^{-1/2}$.

We should expect the optical model used for the derivation of Eq. (3.12) to be valid only when the reduced wavelength $\lambda/2\pi$ of the fields are somewhat smaller than the beam pipe radius a. This means that we should use Eq. (3.12) only for frequencies ω that are at least a few times greater than c/a. Since the wakefields for frequencies lower than the pipe cut-off frequency $\omega_c = 2.4c/a$ arise from trapped resonant modes we would like to define the *diffractive part* as the part due to frequencies greater than ω_c, which is a frequency high enough that

we should expect the optical model – Eq. (3.12) – to apply. So we will assume here that Eq. (3.12) is applicable for all $\omega > \omega_c$.

G. Dôme[3] has derived an analytical approximation for the wakefields of a cavity with beam tubes based on the mode structure of a closed cavity. In the limit of high frequencies his expression for the longitudinal resistance is identical to our result. Recently S. Heifets and S. Kheifets[4] have described a different frequency domain calculation of the longitudinal impedance of a single cavity. Their results also give a smoothed impedance that is in agreement with Eq. (3.12). Note that our result differs from that of the Sessler-Vainsteyn model,[10] which is often used to calculate the impedance of *periodic* structures, and which predicts a high frequency variation of $\mathcal{R}_{\|}(\omega)$ of $\omega^{-3/2}$.

You will notice that the depth b of the cavity does not appear in Eq. (3.12). The reason is that the diffraction model considers only fields generated at the cavity "edge" – where the beam pipe meets the cavity. And we would argue on physical grounds that this limitation is appropriate for the short-time wakefields in which we are interested here. We can understand why by the following qualitative argument. Some of the fields generated when the leading edge of the bunch reaches the entrance to the cavity will propagate out to the outer wall at radius b and then back again to the exit port of the cavity, where they then proceed down the beam pipe. If these fields arrive at the exit port *after* the tail of the bunch has already left the cavity they will never catch up to the bunch, and will never affect the *short-time* part of the wakefields, or the loss factor $k_{\|}$ – which depends only on the wakefields over the bunch. (We are assuming that all bunches have a finite length, and so ignore the theoretically infinite tails that would be present in ideal gaussian bunches. In the later numerical work, the bunches are, in fact,

truncated at $\pm 4\sigma$.) In this case the short-time wakes cannot depend on b. In more quantitative terms, so long as b is sufficiently large that the relation

$$(g + \ell/2)\ell/2 < (b - a)^2 \tag{3.13}$$

holds, with ℓ the total bunch length, we can expect to ignore the effects of a finite cavity depth.

We will define $k_{\|D}(\sigma)$ to be the diffractive part of the loss factor – namely that part of the integral of Eq. (2.6) for which ω is greater than $\omega_c = 2.4c/a$. Then, $k_{\|D}(\sigma)$ is just the $k_{\|2}$ of Eq. (3.6), when we take $\alpha = 1/2$ and $\omega_t = \omega_c$. We find that

$$k_{\|D}(\sigma) = \frac{Z_0 c}{4\pi^{5/2} a}\sqrt{\frac{g}{\sigma}}\left[\Gamma(1/4) - 4\left(\frac{\omega_c \sigma}{c}\right)^{1/2}\right] \qquad (\sigma \text{ small}) \ , \tag{3.14}$$

$(\Gamma(1/4) = 3.63\ldots)$.

We will refer to the *asymptotic form* of the loss factor as the limiting form of Eq. (3.14) as σ goes to zero:

$$k_{\|}(\sigma) = \frac{\Gamma(1/4) Z_0 c}{4\pi^{5/2} a}\sqrt{\frac{g}{\sigma}} \ . \tag{3.15}$$

Note that if we had used the simple approximation Eq. (3.1) for calculating the loss factor, our result would only have changed by 10%.

Since the resistance of Eq. (3.12) falls off more slowly than $1/\omega$ the high frequency impedance will dominate the wake functions at small s. Using Eq. (3.12) for $\mathcal{R}_{\|}(\omega)$, and assuming it is valid for all frequencies, we can take the

inverse transform of Eq. (2.3) to find the asymptotic form of the impulse wake function for small s. We get

$$W_{\|0}(s) = \frac{Z_0 c}{\sqrt{2}\pi^2 a}\sqrt{\frac{g}{s}} \quad . \tag{3.16}$$

Using this form for $W_{\|0}(s)$ in Eq. (2.2) the wake for short gaussian bunches becomes

$$W_{\|}(s,\sigma) = W_{\|0}(\sigma)F(s/\sigma) \quad , \tag{3.17}$$

with the normalized wake function $F(x)$ given by

$$F(x) = \frac{1}{\sqrt{2\pi}}\int_0^\infty \frac{e^{-(y-x)^2/2}}{\sqrt{y}}\,dy \quad . \tag{3.18}$$

A graph of the function $F(x)$ is shown in Fig. 3.

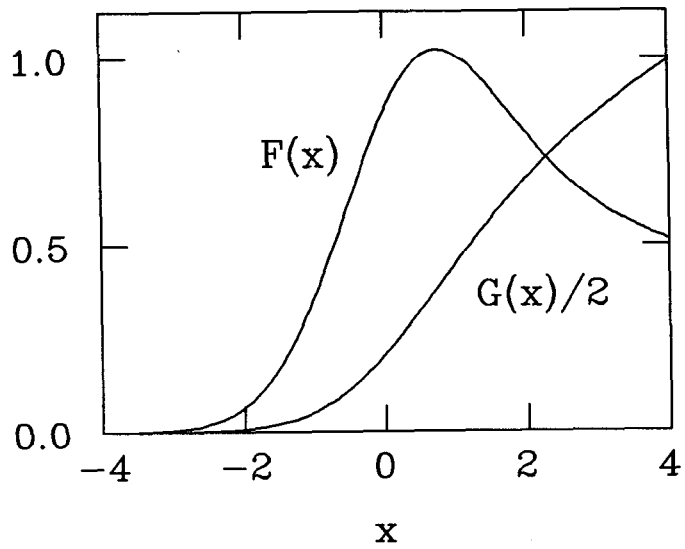

Fig. 3. The normalized asymptotic wake functions F(x) and G(x).

3.4 THE DIFFRACTION MODEL: THE TRANSVERSE WAKES

We show in Appendix A how the diffraction model can be used to derive the transverse resistance $\mathcal{R}_\perp(\omega)$ of a cavity at high frequencies – namely for frequencies somewhat larger than c/a. We find there – see Eq. (A.15) – that

$$\mathcal{R}_\perp(\omega) = \frac{2c}{a^2\omega}\mathcal{R}_\parallel(\omega) \quad . \tag{3.19}$$

This equation is identical to what one finds for a pipe with a short resistive gap. See, for example, F. Sacherer.[11] We should, perhaps, not be too surprised, because the diffractive energy loss mechanism is much like what we would expect for a lossy beam tube. Although Eq. (3.19) has been used to estimate the transverse impedance of a variety of structures when their longitudinal impedance is known, we would emphasize that this equation is not true in general.

We can make use of Eq. (3.19) to obtain some useful relations between the corresponding wake functions for small times. If we multiply both sides of Eq. (3.19) by ω and then take the inverse Fourier-transform we find that the impulse transverse wake $W_{\perp 0}(s)$ is proportional to the integral of the impulse longitudinal wake $W_{\parallel 0}(s)$ for very small s :

$$W_{\perp 0}(s) = \frac{2}{a^2}\int_{-\infty}^{s} W_{\parallel 0}(s')\,ds' \quad . \tag{3.20}$$

Similarly Eq. (3.19) implies also that the transverse wake function $W_\perp(s)$ is proportional to the integral over s of $W_\parallel(s)$ for short bunches:

$$W_\perp(s) = \frac{2}{a^2}\int_{-\infty}^{s} W_\parallel(s')\,ds' \quad . \tag{3.21}$$

If we then make use of Eq. (2.13), we can rewrite the above equation to give the

longitudinal dipole wake function $W_{\parallel}^{(1)}(s)$ in terms of the longitudinal (monopole) wake function $W_{\parallel}(s)$

$$W_{\parallel}^{(1)}(s) = \frac{2}{a^2} W_{\parallel}(s) \quad . \tag{3.22}$$

The diffraction model predicts that the two longitudinal wake functions will have the same form for short bunches.

Using Eq. (3.19) with Eq. (3.12) we can obtain the high frequency dependence of $\mathcal{R}_{\perp}(\omega)$

$$\mathcal{R}_{\perp}(\omega) = \frac{Z_0 \sqrt{g}}{\pi^{3/2} a^3} \left(\frac{c}{\omega}\right)^{3/2} \quad . \tag{3.23}$$

The transverse resistance decreases as $\omega^{-3/2}$ at high frequencies.

As in the longitudinal case we define $k_{\perp D}(\sigma)$, the diffractive part of the transverse impulse factor, as that part of Eq. (2.11) for which $\omega > \omega_c$.* Taking Eq. (3.9) with $\beta = 3/2$ and $\omega_r = \omega_c$ yields

$$k_{\perp D}(\sigma) = \frac{4 Z_0 c}{\pi^3 a^3} \sqrt{g\sigma} \left[f(3/2) - \left(\frac{\omega_c \sigma}{c}\right)^{1/2} \right] \qquad (\sigma \text{ small}) \ , \tag{3.24}$$

(with $f(3/2) = 1.09\ldots$). The asymptotic form of the impulse factor then becomes

$$k_{\perp}(\sigma) \ = 4 f(3/2) \frac{Z_0 c}{\pi^3 a^3} \sqrt{g\sigma} \ = (4.36\ldots) \frac{Z_0 c}{\pi^3 a^3} \sqrt{g\sigma} \quad . \tag{3.25}$$

The transverse impulse factor of a gaussian bunch goes to zero as $\sigma^{1/2}$.

---

* We are aware that the pipe cut-off frequency is different for the transverse and longitudinal waveguide modes; we will, however, use the longitudinal cut-off frequency $\omega_c = 2.4c/a$ as the limit of validity of the diffraction model also for the transverse wakefields.

Combining Eqs. (3.16) and (3.20) we find that the impulse transverse wake is given, for asymptotically small s, by

$$W_{\perp 0}(s) = \frac{2^{3/2} Z_0 c}{\pi^2 a^3} \sqrt{gs} \quad . \tag{3.26}$$

Using this impulse wake, we find the transverse wake function of a short gaussian bunch has the universal form

$$W_\perp(s,\sigma) = W_{\perp 0}(\sigma) G(s/\sigma) \quad , \tag{3.27}$$

in which the normalized wake function $G(x)$ is given by

$$G(x) = \frac{1}{2} \int_0^x F(y)\, dy \quad . \tag{3.28}$$

$G(x)$ is also shown in Fig. 3.

* * *

We note here that the functions $k_\parallel(\sigma)$, $W_{\parallel 0}(s)$, $k_\perp(\sigma)$ and $W_{\perp 0}(s)$ have also been evaluated by Dôme[3] using his resonant mode model; and our results are in accord with his in the limit of small argument – differing only by a few percent in the numerical factors.

4. The Time Domain Computations

The computer program TBCI[1] was used to compute the wakefields, loss factors and transverse impulse factors of short gaussian bunches in the cavity shown in Fig. 1. To be specific, we have chosen the dimensions to represent a typical cell of the SLAC linac structure, namely $g/a = 2.51$ and $b/a = 3.55$.

Computations were done for gaussian bunches with r.m.s. length from $\sigma/a = 0.0086$ to $\sigma/a = 0.172$. (The gaussian distributions were truncated at $\pm 4\sigma$.) We therefore probed the broad-band impedance up to frequencies $\omega \sim 100c/a$. For numerical stability something like six mesh points are needed per σ of length. Therefore the shortest bunch lengths computed required a very large amount of computer memory, as well as lots of CPU time. The longest bunches considered here are those for which the inequality of Eq. (3.13) (taking $\ell = 8\sigma$) is still satisfied for the dimensions of the SLAC structure. So for all the results given here the cavity radius b has no effect on the short range wakefield; the bunch does not know that the outer wall is there. Taking advantage of this fact in order to reduce the number of mesh points required for the shorter bunch lengths, the value of b was adjusted, in the actual computations, to be just large enough that Eq. (3.13) was still satisfied.

4.1 Computations of the Longitudinal Wakes

The computed loss factor $k_{\|}$ for several bunch length is shown by the diamonds in Fig. 4. The solid curve gives the asymptotic results of the diffraction model, Eq. (3.15). We want to emphasize that no normalization factor has been applied to either the computation or theory.

We show by the dotted curve in Fig. 4 the contribution to $k_{\|}(\sigma)$ from the diffractive part of the wakefields, as given the by approximate formula Eq. (3.14). The graph shows that the computed results approach very closely the diffraction asymptote – which varies as $\sigma^{-1/2}$ – as σ/a approaches zero. Indeed it appears that for the bunch lengths considered the asymptotic diffraction formula represents the loss factor rather well – certainly better than we might expect from the diffractive part of the wake alone.

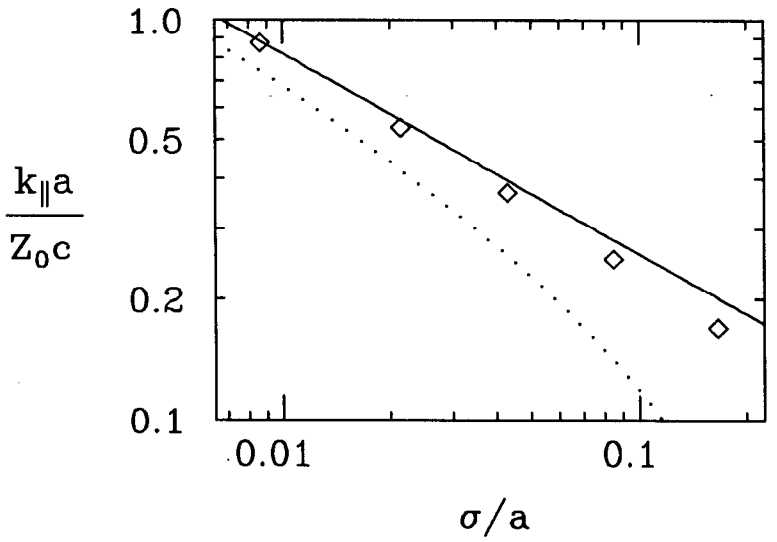

Fig. 4. The loss factor $k_{\|}$ as a function of bunch length σ for our structure (with $g/a = 2.51$). The diamonds display the results computed by TBCI. The solid curve is the diffractive asymptote, Eq. (3.15). The dotted curve shows the contribution of the diffractive part of the wakefields, Eq. (3.14).

T. Weiland has obtained similar results for short bunches using TBCI. He has kindly provided us with his values for $k_{\|}(\sigma)$ for the PETRA cavity with σ/a between 0.033 and 0.33. In this region he finds that $k_{\|}(\sigma)$ follows very closely

the $\sigma^{-1/2}$ dependence we observe.

The computed wake functions $W_{\|}(s,\sigma)$ are plotted in Fig. 5 for gaussian bunches with three different bunch lengths: $\sigma/a = 0.0086$ (dashes), 0.043 (dots) and 0.167 (dotdash). Note that the ordinate is scaled by the factor $(a\sigma)^{1/2}$. The solid curve gives the asymptotic form obtained from the diffraction model, Eq. (3.17). The bunch form is shown in the bottom frame, with the head to the left.

The form of $W_{\|}$ is roughly the same for the three examples. And in more detail, as we move toward the smaller values of σ the curve of $W_{\|}$ does seem to be approaching more closely the asymptotic curve. There appears, however, to be a slight discrepancy between the diffraction asymptote and the direction the numerical results seem to be heading. This discrepancy might be due to the approximate nature of the diffraction model; or it might be due to numerical inaccuracies in the computations.

To find the variation of the loss factor $k_{\|}$ with the cavity gap g, we have computed it with TBCI for several values of g/a, keeping constant a bunch length $\sigma/a = 0.021$. The results are shown in Fig. 6 by the diamonds. The asymptotic dependence of the diffraction model Eq. (3.15) is shown by the solid curve – which varies as $g^{1/2}$. We see that over the calculated range, the computed results also increase very nearly as $g^{1/2}$.

4.2 Computations of the Transverse Wakes

The transverse wakefields of short bunches in our model structure were also computed with the code TBCI. The impulse parameter $k_{\perp}$ is shown for various bunch lengths by the diamonds in the top frame of Fig. 7. The solid line is the diffraction asymptote, Eq. (3.25). The dotted curve shows the diffractive part for

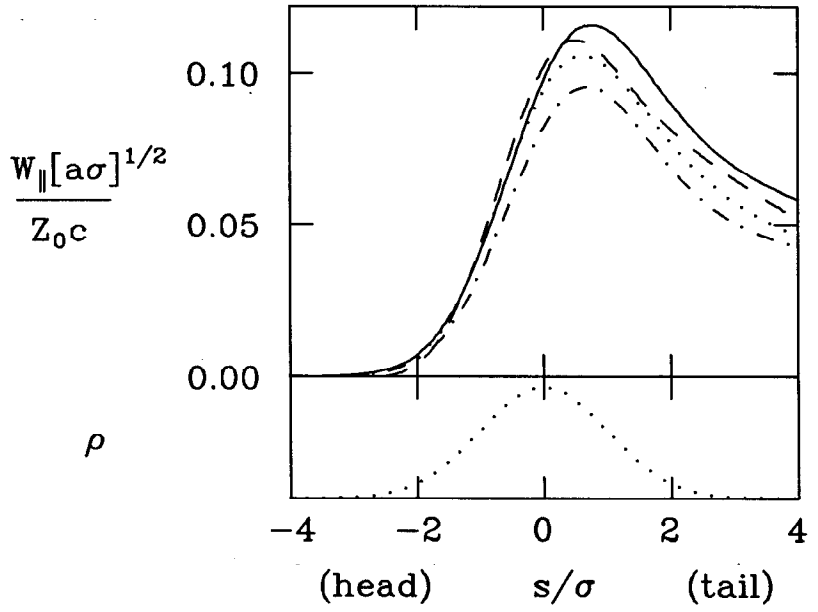

Fig. 5. The wake function $W_\parallel(s,\sigma)$ of a gaussian bunch in our example structure. Results are given for σ/a equals 0.0086 (dashes), 0.043 (dots), and 0.167 (dotdashes), with $g/a = 2.51$. The solid curve gives the diffraction asymptote, Eq. (3.17). The charge distribution is given by the dotted curve in the lower frame, with the head of the bunch to the left.

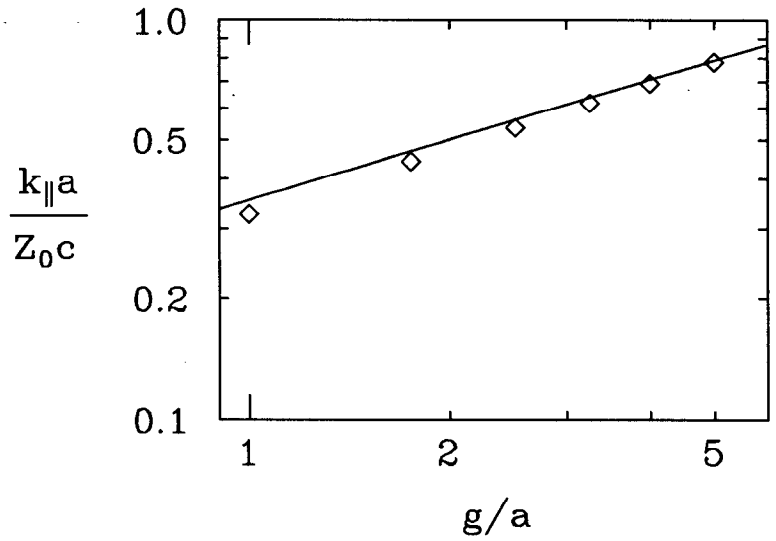

Fig. 6. The loss factor $k_\parallel(\sigma)$ as a function of the gap g for a bunch with $\sigma/a = 0.021$, which corresponds to one of the points in Fig. 4. The diamonds give the results computed by TBCI. The curve gives the diffraction asymptote, given by Eq. (3.15).

each σ, as given by the approximate formula Eq. (3.24). The computed results agree rather well with the diffraction asymptote for small σ. The bottom frame gives the dipole loss factor $k_\parallel^{(1)}$ as function of σ. These curves are very similar in form to those for the monopole loss factor given earlier (see Fig. 4). Note, however, that the scaling in the two graphs differs by the factor $2/a^2$.

The dipole wake function $W_\perp(s,\sigma)$ is shown in Fig. 8 for bunch lengths $\sigma/a = 0.0086$ (dashes), 0.043 (dots) and 0.167 (dotdash). The asymptotic form of the diffraction model is given as the solid curve. The wake form does seem to be approaching the asymptotic one as σ approaches zero. In the middle frame we give the dipole longitudinal wake $W_\parallel^{(1)}$ for these cases. From Eq. (2.13) we know that this function is equal to $dW_\perp/ds$. Note that the structure of these curves is similar to that of the longitudinal wakefields. We may note that the fact that the

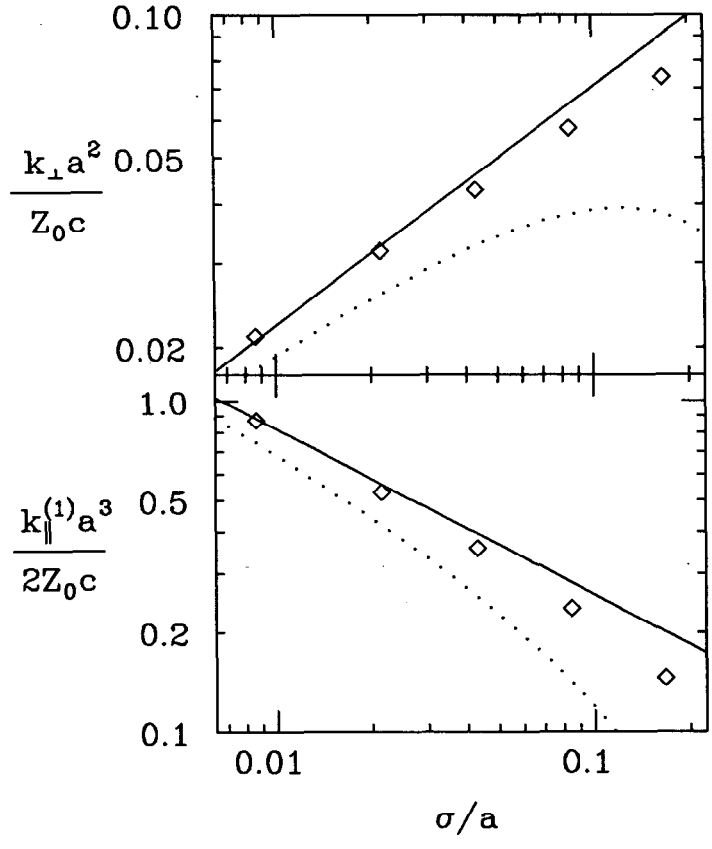

Fig. 7. The functions $k_\perp$ and $k_\parallel^{(1)}$ are shown for various σ/a for our structure with $g/a = 2.51$. The solid curve in the upper frame shows the asymptotic behavior predicted by the diffraction model, Eq. (3.25), and the dotted curve shows the diffractive part of the impulse factor, Eq. (3.24); the curves in the lower frame give their longitudinal counterpart.

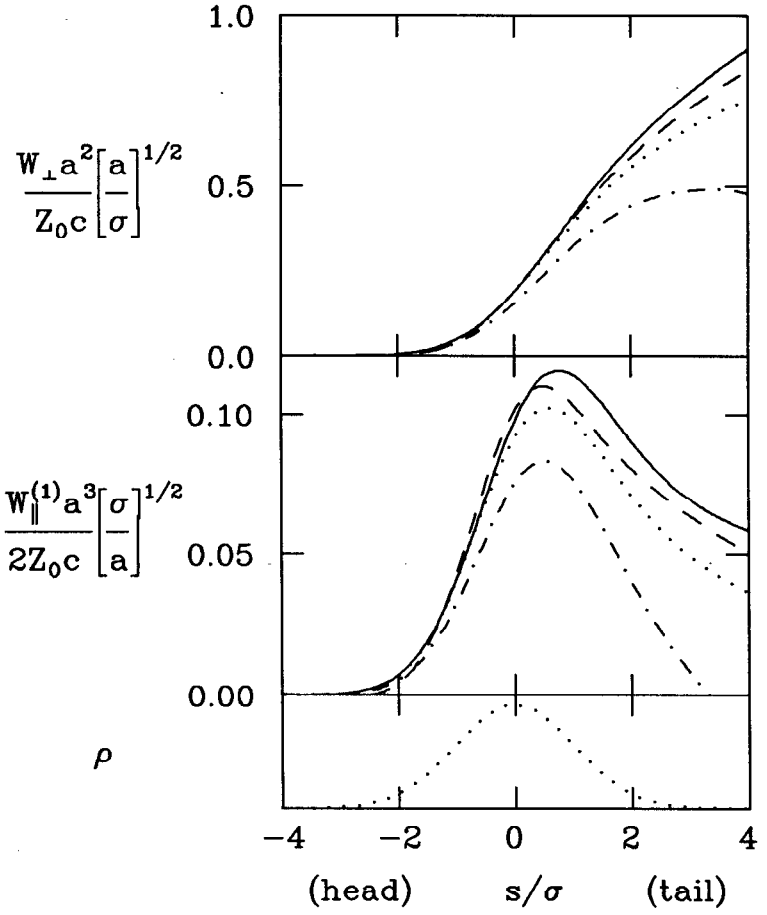

Fig. 8. The transverse wake function $W_\perp(s,\sigma)$ and the dipole longitudinal function $W_\parallel^{(1)}(s,\sigma)$ along a gaussian bunch in our structure. The results are given for $\sigma/a = 0.0086$ (dashes), 0.043 (dots), and $\sigma/a = 0.167$ (dotdashes), with $g/a = 2.51$. The asymptotic diffraction model results, Eq. (3.27), are shown by the solid curves. The charge distribution is given by the dotted curve in the bottom frame.

dipole longitudinal wake function $W_{\parallel}^{(1)}$ approaches, for small σ, the (monopole) wake function $W_{\parallel}$ times $2/a^2$ is rigorously predicted by the diffraction model.

* * *

We should note that V. Balakin and A. Novokhatsky have previously used a time domain code similar to TBCI to investigate the wake functions $W_{\parallel}(s,\sigma)$ and $W_{\perp}(s,\sigma)$ for gaussian bunches with various values of σ/a in a *periodic* structure. Although they have not described their method they report results[12] that resemble ours.

5. Conclusions

The longitudinal and transverse wakefields produced by very short gaussian bunches in an accelerating cavity with infinite beam tubes have been studied using the numerical program TBCI. Calculations were done for bunches with rms bunch length σ ranging from 1/5 to 1/100 of the pipe radius a. In all cases considered the cavity depth b was large enough so that it has no influence on the wakefields at the bunch itself. We presented the computed loss factor $k_{\parallel}(\sigma)$, the longitudinal wake function $W_{\parallel}(s,\sigma)$, the impulse factor $k_{\perp}(\sigma)$ and the transverse wake function $W_{\perp}(s,\sigma)$ for several bunch lengths in our range of interest.

We have also described an analytic model, the "diffraction model", based on an original idea by J. Lawson, which we expect to be applicable for short bunches. The model gives a longitudinal resistance $\mathcal{R}_{\parallel}(\omega)$ that decreases as $\omega^{-1/2}$ at high frequencies and a transverse resistance $\mathcal{R}_{\perp}(\omega)$ that decreases as $\omega^{-3/2}$ – with their ratio equal to $\omega a^2/(2c)$. We note that the high frequency part of the longitudinal impedance predicted by the diffraction model is identical to that given by Dôme, and Heifets and Kheifets.

In order to compare the diffraction model with the TBCI results we have used the high frequency impedances predicted by the model to calculate the asymptotic forms of the loss factor, impulse factor and wake functions for small σ. Because we expect the wakefields to be accurately described by the diffraction model only for frequencies ω greater than a few times c/a, we have also obtained from the model an estimate of what we call the "diffractive part" of the wakefields, namely the contribution to the bunch factors and wake functions from frequencies above a cut-off frequency which we take equal to $\omega_c = 2.4c/a$.

We find that the bunch factors and wake functions obtained by TBCI agree very well with the diffraction model for the shortest bunch lengths studied. For the longer bunch lengths the TBCI results still continue to follow rather closely the power dependence of the asymptotic forms obtained from the diffraction model. This result is somewhat surprising to us since our estimate of that part of the wake functions contributed by the "diffractive part" of the wakefields begins to fall noticeably below the asymptotic form for the longer bunch lengths studied.

We have also confirmed that at short bunch lengths the loss factor $k_{\|}(\sigma)$ obtained from TBCI is proportional to the square-root of the cavity gap g, as predicted by the diffraction model.

Finally we may mention that in our computations of the transverse wakes we have also obtained the the longitudinal dipole wake function $W_{\|}^{(1)}(s,\sigma)$, and have found that it approaches $2/a^2$ times the longitudinal wake function $W_{\|}(s,\sigma)$ for small bunches, as predicted by the diffraction model.

ACKNOWLEDGEMENTS

We have profited from discussions on the subject of wakefields with S. Kheifets, A. Novokhatsky, J. Rees and P. Wilson.

APPENDIX A

The Diffraction Model for Short-Time Wakes

In 1968 J. Lawson[2] proposed a method for estimating the energy loss of a point-like bunch in passing through an accelerating cavity by drawing on the results of optical diffraction theory. We have adapted Lawson's method for calculating the high-frequency behavior of the wakefields of a cavity. The results are expected to be reliable for the diffractive part of the wakefields – namely for the contribution from frequencies somewhat higher than the cut-off frequency ω_c of the beam tube.

Lawson considered only the special case of the total energy lost by a *point* bunch, and his result is therefore only applicable for bunch lengths σ that are less than a/γ – where a is the radius of the beam tube. We may call this the "low-energy regime". We, on the other hand, are interested here only in the "high-energy regime", in which the bunch is much longer than a/γ – although still less than a itself. We have adapted Lawson's ideas to obtain the smoothed high-frequency behavior of the longitudinal resistance $\mathcal{R}_{\|}(\omega)$ and of the transverse resistance $\mathcal{R}_{\perp}(\omega)$. Our results differ importantly from Lawson's in that the γ dependence found in his result is no longer present.

A.1 THE DIFFRACTION MODEL

We consider the geometry shown in Fig. 10. A particle bunch travels along the axis of a perfectly conducting cylindrical beam pipe of radius a and passes through a cavity gap of length g before re-entering the beam pipe. We assume that for the bunch lengths of interest here the outer wall of the cavity is far enough away that it can be ignored.

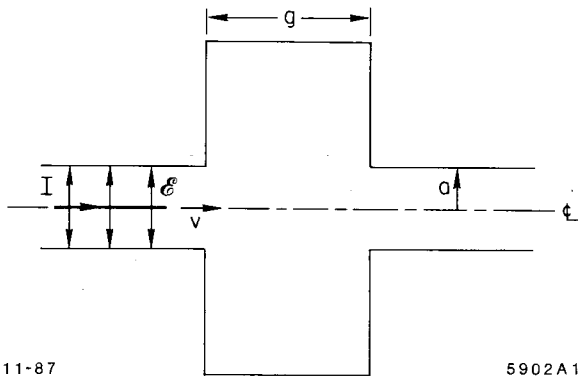

Fig. 10. An ultra-relativistic bunch enters a cavity with gap g and tube radius a.

In the beam pipe the bunch is accompanied by an electric field $\mathcal{E}$ which we may take to be radial and proportional to the instantaneous bunch current. This assumption is justified provided that we are in the high-energy regime defined above. This restriction is not necessary but is convenient for the present purposes. Then Gauss's Law gives us that the electric field at the wall $\mathcal{E}_a$ is related to the local bunch current I by

$$\mathcal{E}_a = \frac{Z_0 I}{2\pi a} \quad , \tag{A.1}$$

with $Z_0 = 1/\epsilon_0 c$, the "characteristic impedance" of the vacuum. The associated magnetic field at the wall B_a is azimuthal and of magnitude $\mathcal{E}_a/c$, so the electric

and magnetic fields at the wall look, locally, just like those in a free plane wave.

Lawson's proposal was that for high frequencies, the spreading of the electromagnetic fields in the cavity gap should be just as would occur when a plane wave passes an obscuring edge, so that we may use the classical diffraction theory of optics to calculate the spreading fields. Clearly, we may only expect this assumption to be reasonable for reduced wavelengths in the field somewhat shorter than the pipe radius a – meaning for bunch frequencies ω somewhat greater than c/a. For these frequencies we may consider the diffracted fields associated with some small azimuthal segment of the edge of the gap in Fig. 1 to correspond closely to those in an optical wave which is diffracted by a screen with a straight edge.

The diffraction geometry is sketched in Fig. 11. A monochromatic plane wave of intensity J_0 – which we may take as the time-averaged Poynting vector – is incident perpendicular to an obscuring screen with a straight edge. The intensity J of the diffracted wave observed at a point P, which is at a distance g beyond the screen, varies with the distance y from the edge of the geometric shadow as sketched in the graph in Fig. 11. The relative intensity J/J_0 is $1/4$ at the edge, falls to zero inside the shadow, and approaches 1 asymptotically in the non-shadow region. The characteristic scale of the variation of J with y is of the order of $\sqrt{\lambda g}$ where λ is the wavelength of the free wave.

According to standard diffraction theory[13] the intensity on the plane at g depends on the transverse position y only through a single dimensionless parameter u which we can take as

$$u = \sqrt{\frac{2}{\lambda g}}\, y \quad . \tag{A.2}$$

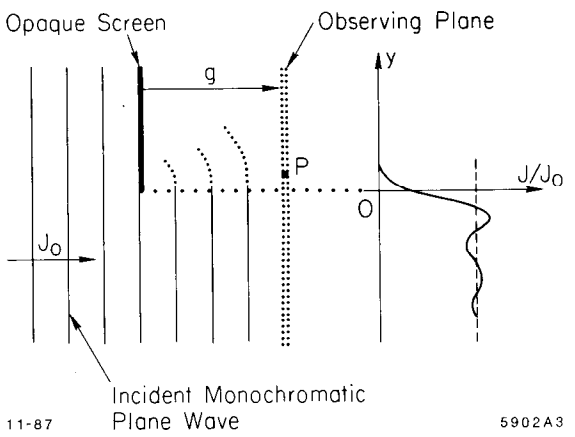

Fig. 11. The diffraction geometry.

The intensity at y can then be written as

$$\frac{J(y)}{J_0} = F(u) = \frac{1}{2}[(C(u) - 1/2)^2 + (S(u) - 1/2)^2] \quad , \qquad \text{(A.3)}$$

where $C(u)$ and $S(u)$ are the Fresnel Integrals.

Lawson then proposed that the energy diffracted into the geometric shadow in Fig. 11 corresponds to the energy deposited in the cavity of Fig. 10, and thus gives us the energy lost by the beam. *Except for a factor of two!* In addition to the loss into the cavity there is also a loss into diffractive fields that propagate down the beam pipe. It is these fields which, interfering with the undiffracted wave, give rise to the oscillations of J/J_0 in the region just outside the geometric shadow. From a well-known scattering theorem – which in optics is a consequence of Babinet's Principle – the two parts of the diffracted fields carry equal energy. The total energy diffracted is twice the energy diffracted into the shadow.

Consider now a segment $\Delta\ell$ of the edge of the screen in Fig. 11 (taken perpendicular to the plane of the figure). We may think that the power ΔP_D diffracted by this segment is given by twice the integral of J over a strip of width

$\Delta\ell$, extending from $y = 0$ to $y = \infty$. Namely,

$$\Delta P_D = 2\Delta\ell \int_0^\infty J(y)\, dy = \Delta\ell J_0 \sqrt{2\lambda g} \int_0^\infty F(u)\, du \quad . \tag{A.4}$$

The integral of the Fresnel function $F(u)$ is just equal to[14] $1/(2\pi)$. Then, replacing λ by $2\pi c/\omega$ we find that

$$\Delta P_D = \sqrt{\frac{cg}{\pi\omega}} J_0\, \Delta\ell \quad . \tag{A.5}$$

A.2 The Longitudinal Resistance

We are now in a position to look at the diffractive energy loss by a beam. In the situation sketched in Fig. 10, when there is a sinusoidal beam current $I(\omega)$ the Poynting vector at the wall is (using Eq. (A.1))

$$J_0 = \frac{\langle \mathcal{E}_a^2 \rangle}{Z_0} = \frac{Z_0 \langle I^2(\omega) \rangle}{4\pi^2 a^2} \quad , \tag{A.6}$$

where the pointed brackets indicate a time average. Putting this intensity into Eq. (A.5), we get the power diffracted by each element $\Delta\ell$ of the perimeter of the cavity opening. Adding up the contributions from the full perimeter of length $2\pi a$, we get a total diffracted power at ω of

$$P_D(\omega) = \frac{Z_0}{2\pi^{3/2}} \sqrt{\frac{cg}{a^2\omega}} \langle I^2(\omega) \rangle \quad . \tag{A.7}$$

The ratio of $P_D(\omega)$ to $\langle I^2(\omega) \rangle$ is the resistive part $\mathcal{R}_\parallel(\omega)$ of the longitudinal cavity impedance; so we find that

$$\mathcal{R}_\parallel(\omega) = \frac{Z_0}{2\pi^{3/2}} \sqrt{\frac{cg}{a^2\omega}} \quad . \tag{A.8}$$

At high frequencies the longitudinal resistance varies as $\omega^{-1/2}$. As discussed in

the body of the report, this result is identical to results obtained by others using widely different methods.

A.3 The Transverse Resistance

The diffraction model can be extended to obtain also the transverse wake impedance for short bunches. As we will see, the model gives easily the dipole longitudinal resistance $\mathcal{R}_{\parallel}^{(1)}(\omega)$ defined in Section 2.2. We can then use Eq. (2.15) to get $\mathcal{R}_{\perp}(\omega)$.

Consider a horizontal dipole current of strength Id on the central beam line. By a dipole current we mean a positive current I, together with an equal negative current $(-I)$, separated by the small distance d. Then $\mathcal{R}_{\parallel}^{(1)}(\omega)$ is equal to the ratio of $P_D^{(1)}(\omega)$, the power dissipated by a sinusoidal dipole current, to the mean square of the dipole current strength

$$\mathcal{R}_{\parallel}^{(1)}(\omega) = \frac{P_D^{(1)}(\omega)}{\langle I^2(\omega) d^2 \rangle} \quad . \tag{A.9}$$

Here we take that the total power loss is just that into the diffracted fields.

So long as the reduced wavelength c/ω is noticeably smaller than the pipe radius a, we can consider that the power diffracted by each element Δl of the perimeter of the cavity edge is determined only by the local field strength $\mathcal{E}_a$ at that element. For a dipole beam, Eq. (A.1) gets replaced by

$$\mathcal{E}_a^{(1)} = \frac{Z_0}{2\pi} Id \cos\theta \quad , \tag{A.10}$$

where θ is the azimuthal angle from the dipole axis. Then the diffracted power $\Delta P_D^{(1)}(\theta)$ at an element Δl of the edge is given in terms of $\Delta P_D^{(0)}$ the power for

a simple beam current I (a "monopole" beam) by

$$\Delta P_D^{(1)}(\theta) = \left(\frac{2d\cos\theta}{a}\right)^2 \Delta P_D^{(0)} \quad . \tag{A.11}$$

Integrating around the perimeter, we get the total dipole power in terms of the monopole power

$$P_D^{(1)} = \frac{2d^2}{a^2} P_D^{(0)} \quad . \tag{A.12}$$

It follows that $\mathcal{R}_\parallel^{(1)}(\omega)$ is given in terms of the monopole resistance $\mathcal{R}_\parallel^{(0)}(\omega)$ by

$$\mathcal{R}_\parallel^{(1)}(\omega) = \frac{2}{a^2}\mathcal{R}_\parallel^{(0)}(\omega) \quad . \tag{A.13}$$

Taking $\mathcal{R}_\parallel^{(0)}$ from Eq. (A.8), we get that

$$\mathcal{R}_\parallel^{(1)}(\omega) = \frac{Z_0}{\pi^{3/2}a^3}\sqrt{\frac{cg}{\omega}} \quad . \tag{A.14}$$

Alternatively, using Eq. (2.15) to relate $\mathcal{R}_\parallel^{(1)}$ to $\mathcal{R}_\perp$, we find that

$$\mathcal{R}_\perp(\omega) = \frac{2c}{a^2\omega}\mathcal{R}_\parallel(\omega) \quad , \tag{A.15}$$

from which

$$\mathcal{R}_\perp(\omega) = \frac{Z_0\sqrt{g}}{\pi^{3/2}a^3}\left(\frac{c}{\omega}\right)^{3/2} \quad . \tag{A.16}$$

The transverse resistance drops off as $\omega^{-3/2}$ – one power of ω faster than $\mathcal{R}_\parallel(\omega)$. Note that Eq. (A.15) for the relation between $\mathcal{R}_\perp(\omega)$ and $\mathcal{R}_\parallel(\omega)$ is identical to what one finds for a pipe with a short resistive gap. See, for example, F. Sacherer.[11]

REFERENCES

1. T. Weiland, DESY **82**-015 (1982) and *Nucl. Instr. Meth.* **212**, 13 (1983).
2. J. Lawson, Rutherford High Energy Laboratory Report RHEL/M 144 (1968).
3. G. Dôme, *I.E.E.E. Trans. Nucl. Sci.*, NS-32, 2531 (1985).
4. S. Heifets and S. Kheifets, "High-Frequency Limit of the Longitudinal Impedance", CEBAF TN-0063 (1987); to be published in Particle Accelerators.
5. R. B. Palmer, SLAC-PUB-3838 (1986) and Proceedings of Seminar on New Techniques for Future Accelerators, Erice, 1986.
6. J. Rees, SLAC-PUB-4073 (1986) and Proceedings of Advanced Study Institute on Techniques and Concepts of High Energy Physics, St. Croix, 1986.
7. K. Bane, T. Weiland, P. B. Wilson, in *Physics of High Energy Particle Accelerators*, AIP Conf. Proc. No. 127, (Am. Inst. of Physics, New York, 1983), pp. 875-928.
8. See for example P. B. Wilson in *Physics of High Energy Particle Accelerators*, AIP Conf. Proc. No. 87, (Am. Inst. of Physics, New York, 1982), pp. 450-582.
9. W. K. H. Panofsky and W. A. Wenzel, *Rev. Sci. Instrum.* **27**, 967 (1956).
10. E. Keil, *Nucl. Instr. Meth.* **100**, 419 (1972); K. Bane and P. B. Wilson, Proceedings of the 11^{th} Int. Conf. on High Energy Accelerators, CERN (Birkhäuser Verlag, Basel, 1980), p. 592; D. Brandt and B. Zotter, CERN ISR/TH/82-13 (1982).

11. F. Sacherer, CERN Report 77-13, 198 (1977).

12. V. Balakin and A. Novokhatsky, "Beam Dynamics in the VLEPP Linear Accelerator", Int. Conf. on High-Energy Accelerators, Novosibirsk (1986).

13. See, for example, M. Born and E. Wolf, *Principles of Optics*, (Pergamon, Oxford, England, 1980), 6th ed., Chap. 8.

14. See, for example, M. Abramowitz and A. Segun, *Handbook of Mathematical Functions*, (Dover, New York, 1965), p. 303, Eq. 7.4.31.